ARTICLE

Preparation and Acid Catalytic Activity of TiO_2 Grafted Silica MCM-41 with Sulfate Treatment

Dai-shi Guo[a], Zi-feng Ma[a]*, Chun-sheng Yin[b], Qi-zhong Jiang[a]

a. Department of Chemical Engineering, Shanghai Jiao Tong University, Shanghai 200240, China;
b. School of Environmental Science and Engineering, Shanghai Jiao Tong University, Shanghai 200240, China

(Dated: Received on March 14, 2007; Accepted on July 20, 2007)

TiO_2 grafted silica MCM-41 catalyst with and without sulfate treatment were prepared. The structural and acid properties of these materials were investigated by XRD, N_2 adsorption-desorption, element analysis, thermal analysis, Raman and FTIR measurements. Their acid-catalytic activities were evaluated using the cyclization reaction of pseudoionone. It was found that the obtained materials possess well-ordered mesostructure, and the grafted TiO_2 components were in highly dispersed amorphous form. T/MCM41 without sulfation contained only Lewis acid sites, while Brønsted and Lewis acidities were remarkably improved for the sulfated materials ST/MCM41 and d-ST/MCM41. T/MCM-41 was not active for the cyclization reaction of pseudoionone, but ST/MCM-41 and d-ST/MCM-41 possessed favorable catalytic activities. The catalytic performance of ST/MCM-41 was comparable with that of the commercial solid acid catalyst of Amberlyst-15, and better than that of d-ST/MCM-41, although the latter underwent a second TiO_2 grafting process and accordingly had higher Ti and S content. The specific surface structure of Si−O−Ti−O−S=O in ST/MCM-41 and the bilateral induction effect of Si and S=O on Si−O−Ti bonds were speculated to account for its higher acid catalytic activity.

Key words: TiO_2 grafting, Sulfate treatment, Silica MCM-41, Acid catalytic activity, Cyclization of pseudoionone

I. INTRODUCTION

TiO_2-SiO_2 mixed oxides have attracted extensive attention due to their intriguing features and potential applications in heterogeneous catalysis resulting from the interaction of the two important oxides [1,2]. Sulfate treatment of the TiO_2-SiO_2 mixed oxides with various TiO_2 content have been carried out, in order to investigate the surface acidity and acid-catalytic activity as obtained after the introduction of inductive effect of S=O in the cases of sulfated metal oxides [3-5]. From the structural point of view, the sulfated TiO_2-SiO_2 does not have ordered pores and favorable surface area, and additionally only the exposed Ti sites on surface are accessible for catalysis. In recent years, chemical grafting technique was applied to incorporate highly dispersed TiO_2 onto pore surfaces of various mesoporous silica [6-13]. The obtained materials have well-ordered mesostructure and large surface area. Though the Ti content in these materials is low, the TiO_2 components are all located on the silica pore surface via chemical Si−O−Ti bonds, and mainly in isolated tetrahedrally coordinated units, therefore the materials possess much more regular structure of active sites on surface than TiO_2-SiO_2 mixed oxides. Nevertheless, these materials were usually used without sulfate treatment, and only for photocatalysis and epoxidation catalytic reactions [6-10]. To date, fewer studies have been carried out on their sulfated form and applications as solid acid catalysts.

The ionone isomers are of both academic and commercial value, and have been widely used as fragrance, starting materials or building blocks in synthesis of medicine and many kinds of fine products [14]. Ionones are usually produced via the cyclization reaction of pseudoionone, and this reaction is conventionally catalyzed by concentrated liquid acids [15], which unfortunately leads to subsequent separation difficulties, operation inconvenience, and environmental pollutions. To avoid all the problems of the reaction caused by the use of liquid acid catalysts, the employment of solid acid catalysts is an efficient method. However, research work on solid acid catalyzed cyclization reactions of pseudoionone are still scarce until now. It has been known that sulfated metal oxides show remarkable catalytic activities for various reactions [16]. In order to provide large surface area and easy accessibility to the active sites for the bulky reactant molecules, such as pseudoionone in this case, efforts have been carried out to provide sulfated metal oxides with ordered mesostructure [17-19], but this was mainly achieved by supporting the catalysts onto mesoporous silica rather than surface grafting modification. The sulfated version of TiO_2 modified mesoporous silica can be expected to possess potentially structural and acidic advantages for catalysis of the reaction as a new solid catalyst.

Considering the insufficient research work in TiO_2

*Author to whom correspondence should be addressed. E-mail: zfma@sjtu.edu.cn, Tel: +86-21-54742894

modified mesoporous silica materials and solid acid catalysis of cyclization reaction of pseudoionone to ionone, TiO_2 grafted silica MCM-41 with sulfate treatment were developed and investigated in the present work. The pore surface of silica MCM-41 was modified with different amounts of TiO_2 via a consecutive procedure [8], and then promoted with H_2SO_4 solution. TiO_2 grafted MCM-41 without sulfation was also prepared for comparison. The influence of sulfate treatment on the structure, acidity and acid-catalytic activity of TiO_2 grafted MCM-41 was investigated. The structural and acid properties of the obtained materials were characterized with XRD, N_2 adsorption-desorpion, TG-DTG, Raman and FTIR spectroscopy. The acid-catalytic activity of the materials was evaluated with the cyclization reaction of pseudoionone, and that of the commercial acid resin Amberlyst-15 was also tested as a reference catalyst. The generation of acid activity of TiO_2 grafted silica MCM-41 by sulfate treatment was discussed.

II. EXPERIMENTS

A. Samples preparation

The silica MCM-41 was synthesized following the method proposed in the literature [20]. The TiO_2 modification of MCM-41 was performed under nitrogen protection with $Ti(OBu^n)_4$ as grafting agent. A 5.0 g of calcined MCM-41 was placed in a mixed solution of 25 g excess $Ti(OBu^n)_4$ (ca. 5.0 eq. Ti per Si−OH group) and 250 mL *n*-hexane. The mixture was stirred and refluxed at 70 °C for 24 h under protection of nitrogen flow, to ensure that all of the free Si−OH groups could be accessible to the grafting reaction. The solid with Si−O−Ti−OBu groups formed on silica wall surface was washed with anhydrous ethanol repeatedly to remove residual $Ti(OBu^n)_4$ in the mesopores thoroughly. Both the *n*-hexane and anhydrous ethanol were dehydrated with 4A zeolite previously. The washed and filtered solid was dried at 70 °C under vacuum condition (0.06 Pa), then hydrolyzed by stirring in 100 mL deionized water at room temperature for 2 h to generate Si−O−Ti−OH species on the silica wall. The filtered solid was finally treated overnight at 90 °C in a vacuum drying oven. The second grafting of TiO_2 onto the newly formed surface Ti−OH groups was carried out with a part of the solid obtained, using the same procedure mentioned above.

The solids without and with a second TiO_2 grafting treatment were impregnated in 0.5 mol/L H_2SO_4 solution for 1 h, filtered and dried overnight at 90 °C, and then calcined in air atmosphere at 450 °C for 3 h to obtain ST/MCM-41 and d-ST/MCM-41, respectively. TiO_2 modified MCM-41 without a second grafting process and sulfate treatment (T/MCM-41) was obtained by direct calcinations of the hydrolyzed solid at 450 °C for 3 h.

B. Characterization

The XRD patterns were collected on Shimadzu XRD-6000 diffractometer with Ni-filtered CuKα radiation operating at 40 kV and 30 mA. The 2θ range was from 1.0° to 10° and 20° to 70° for characterization of the mesoporous structure and crystalline phase of the grafted TiO_2, respectively. N_2 adsorption-desorption isotherms were measured with Quantachrome NOVA 1000 at 77 K. The samples were outgassed at 300 °C for 3 h before measurement. The specific surface area A of the samples was determined using the BET equation. Since it is impossible to use BJH method to calculate the pore size distribution for the silica MCM-41 sample synthesized in this method, the average pore diameter d was calculated with the formula $d=4V_p/A$, where V_p is the pore volume [20]. Weight loss and derivative weight curves of the samples were recorded on a Perkin-Elmer 7 Series thermogravimetric analyzer with a heating rate of 20 °C/min in a nitrogen flow of 40 cm^3/min. FTIR spectra were recorded with Nicolet Avartar 360 spectrometer. KBr pellets (1% samples and 99% KBr) were used to characterize the formation of Si−O−Ti bonds after TiO_2 grafting treatment, while the spectra of surface S=O vibration resulting from sulfate promotion, as well as that of pyridine adsorption were collected from self-supporting wafers pressed with the prepared samples directly. The wafers were evacuated at 400 °C for 3 h in an *in situ* cell under vacuum at 0.06 Pa and scanned for the characteristis S=O vibration of sulfated metal oxides, then an excess pyridine was injected and adsorbed at room temperature. After evacuation at 200 °C for 30 min, the spectra of pyridine adsorption were collected to identify the presence of Brϕnsted and Lewis acid sites. The Raman spectra were measured using a LabRAM-1B spectrometer with 632.8 nm excitation sources under ambient conditions. Ti content of the samples was analyzed with IRIS ADVANTAGE/1000 ICP-AES, and S content was determined with PE 2400II CHNS/O Analyzer.

C. Catalytic performance test

The cyclization reaction of pseudoinone was carried out in a 100 mL flask reactor. The reactant (1.5 g of pseudoionone) and the solvent (20 mL of toluene) were introduced into the reactor. When the temperature was raised to 100 °C, 1.0 g of the samples was added under constant stirring. The reaction mixture was analyzed on an Agilent 6890N gas chromatograph equipped with FID detector and a 30 m×320 μm×0.25 μm quartz capillary column of HP-5.

III. RESULTS AND DISCUSSION

XRD patterns of the samples are presented in Fig.1. The three peaks of MCM-41 at low diffraction angles show its long-range ordered hexagonal mesostructure

DOI:10.1088/1674-0068/21/01/21-26

TABLE I Physico-chemical properties of the samples

Samples	BET surface area/(m^2/g)	Pore volume/(mL/g)	Average pore size/nm	Ti content/%	S content/%
MCM-41	1226	0.74	2.41	–	–
T/MCM-41	816	0.47	2.31	4.28	–
ST/MCM-41	823	0.49	2.38	4.24	0.87
d-ST/MCM-41	711	0.39	2.29	7.17	2.38

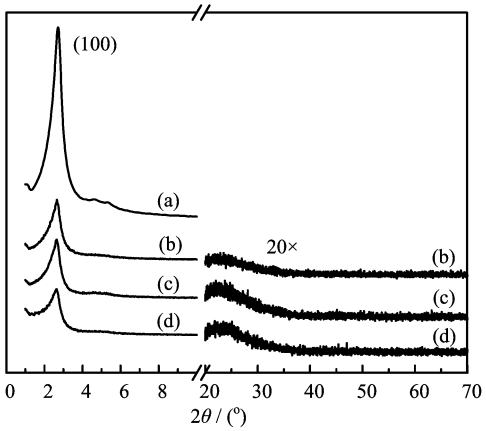

FIG. 1 XRD patterns of (a) MCM-41, (b) T/MCM-41, (c) ST/MCM-41, and (d) d-ST/MCM-41.

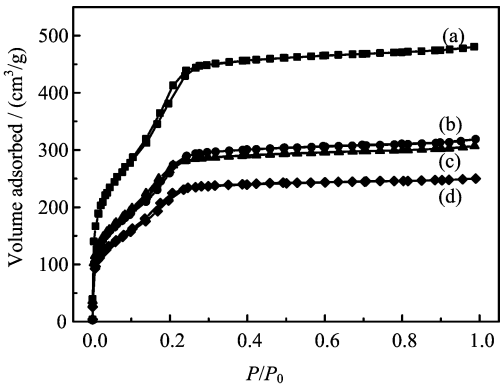

FIG. 2 N_2 adsorption-desorption isotherms of (a) MCM-41, (b) ST/MCM-41, (c) T/MCM-41, and (d) d-ST/MCM-41.

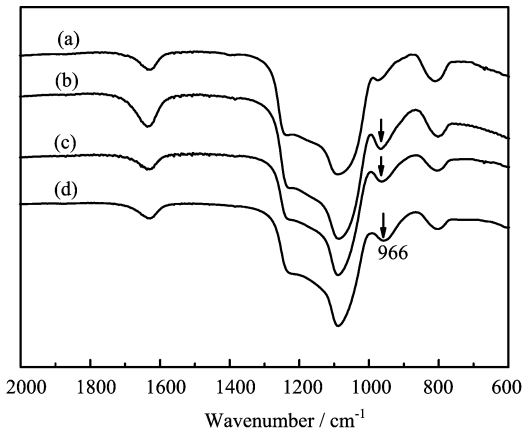

FIG. 3 FTIR spectra of (a) MCM-41, (b) T/MCM-41, (c) ST/MCM-41, and (d) d-ST/MCM-41.

[20]. For T/MCM-41, ST/MCM-41, and d-ST/MCM-41, the weak intensity of the main reflection (100) peak suggests a decreased long-range order of the mesopores resulting from the Ti grafting treatment, while the ordered mesoporous structure of the samples is still kept well. At 2θ range from 20° to 70°, no peaks corresponding to the presence of anatase TiO_2 were detected, which indicates that the grafted TiO_2 is generally in highly dispersed amorphous form rather than crystalline phase.

The N_2 adsorption-desorption isotherms are illustrated in Fig.2, and the physico-chemical properties of the samples are summarized in Table I. The steep inflections in Fig.2 at relative pressure between P/P_o=0.15 and 0.25 show that all the samples have typical mesoporous structures, in good agreement with the results reported by Grün *et al.* [20]. From Fig.2 and Table I, the BET surface area and the total pore volume of the samples decreased successively with the consecutive TiO_2 grafting onto MCM41 mesopores. Meanwhile the average pore size shrunk slightly. It also can be found in Table I that the structural parameters of ST/MCM-41 by N_2 adsorption-desorption measurement are a little better than those of T/MCM-41, which suggests that H_2SO_4 treatment is structurally beneficial to some extent.

FTIR and Raman spectroscopy were used to investigate the surface TiO_2 species. The FTIR spectra are presented in Fig.3. The bands at 966 cm^{-1} can be assigned to the formation of chemical Si−O−Ti bonds [1], which indicates the successful grafting of TiO_2 onto the silica wall of MCM-41. Figure 4 shows the Raman spectra of the samples. The absorbances in 950-1080 cm^{-1} region additionally confirmed the formation of Si−O−Ti structure [1]. For T/MCM-41, the very sharp band at 151 cm^{-1}, and those at 386, 412, 515, and 637 cm^{-1} reveal the presence of anatase phase or TiO_2 polymerization [1,11,12], but which should be a minor part of the surface TiO_2, since no corresponding anatase peaks were detected by XRD in Fig.1. As contrast, the very weak band at 139 cm^{-1} for ST/MCM-41 indicates the absence of anatase phase and serious TiO_2 polymerization after sulfate treatment. According to the data in Table I, the Ti surface concentration

DOI:10.1088/1674-0068/21/01/21-26

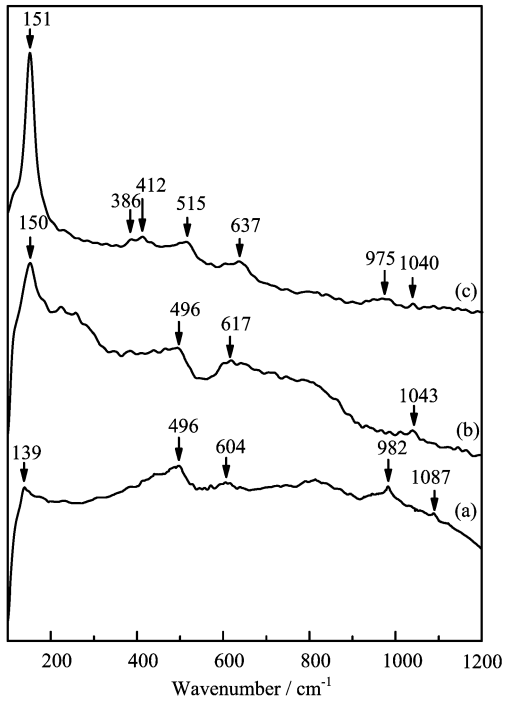

FIG. 4 Raman spectra of (a) ST/MCM-41, (b) d-ST/MCM-41, and (c) T/MCM-41.

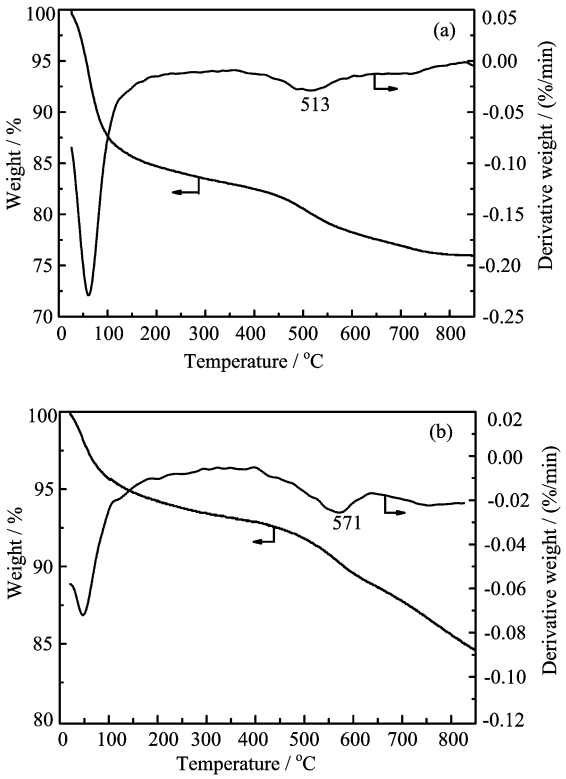

FIG. 5 TG-DTG curves of (a) ST/MCM-41 and (b) d-ST/MCM-41.

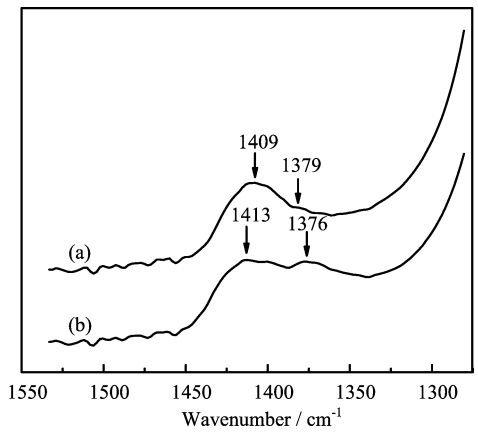

FIG. 6 *In situ* FTIR spectra for S=O vibrations of (a) ST/MCM-41 and (b) d-ST/MCM-41 after evacuation at 40 °C for 3 h.

in ST/MCM-41 is calculated to be only ca. 0.8 nm^{-2}, and the grafted TiO_2 should be generally isolated units in tetrahedral coordination on the silica surface. The band at 1500 cm^{-1} in the spectrum of d-ST/MCM-41 with a higher Ti content is much less intense as compared to T/MCM-41, and most probably corresponding to Ti−O−Ti connectivity resulting from the second TiO_2 grafting process. The two bands of 496 and 617 cm^{-1} for the sulfated samples of ST/MCM-41 and d-ST/MCM-41 can be assigned to a silica framework [11]. It can be concluded from the Raman spectra that the sulfate treatment efficiently restrained the formation of anatase phase and polymerization of TiO_2 on pore surface of silica MCM-41, and the grafted TiO_2 are mainly in the form of isolated units.

According to Table I, d-ST/MCM-41 possesses a much higher S content than ST/MCM-41, indicating that a second Ti grafting process is favorable for improvement of surface S containment. SO_4^{2-} species over the pore surface of ST/MCM-41 and d-ST/MCM-41 were investigated with thermal analysis and *in situ* FTIR spectroscopy. The TG-DTG curves are shown in Fig.5. The weight loss below 100 °C is due to the desorption of physically adsorbed water molecules, while the DTG peaks above 500 °C correspond to the loss of surface S content, suggesting the strong interaction between SO_4^{2-} and pore surface. The characteristic S=O vibration of sulfated metal oxides were measured with *in situ* FTIR, and the spectra are illustrated in Fig.6. ST/MCM-41 showed a band at 1409 cm^{-1} and a shoulder at 1379 cm^{-1}, and d-ST/MCM-41 gave two bands at 1413 and 1376 cm^{-1}, corresponding to the covalent S=O vibration induced from the SO_4^{2-} chelating structures on SO_4^{2-}/SiO_2 and SO_4^{2-}/TiO_2 surface, respectively [21]. The presence of S=O vibration band of SO_4^{2-}/SiO_2 is due to the chelation of SO_4^{2-} onto the hydrogen-bonded Si−OH groups on the silica pore surface of TiO_2 modified MCM-41, which were inert to grafting reagents and retained on the surface after TiO_2 modification [22].

The pyridine adsorption spectra by using *in situ*

DOI:10.1088/1674-0068/21/01/21-26

TABLE II Catalytic activity of the cyclization reaction of pseudoionone over the samples

Reaction time/min	T/MCM-41		ST/MCM-41		d-ST/MCM-41		Amberlyst-15	
	Conv.[a]/%	Selec.[b]/%	Conv./%	Selec./%	Conv./%	Selec./%	Conv./%	Selec./%
30	0.00	–	78.68	39.36	57.04	29.47	76.84	39.61
60	0.38	–	87.01	41.24	73.61	32.74	90.19	38.72
90	1.18	–	92.08	41.41	78.44	33.08	95.81	38.32
120	2.02	–	96.31	42.04	82.16	34.46	97.71	35.53

[a] Conv. refers to Conversion.
[b] Selec. refers to Selectivity.

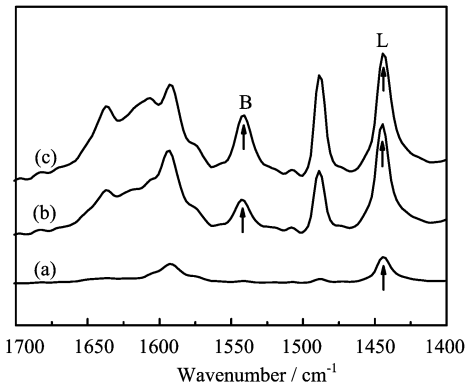

FIG. 7 *In situ* pyridine adsorption FTIR spectra measured at 200 °C of (a) T/MCM-41, (b) ST/MCM-41, and (c) d-ST/MCM-41. L refers to Lewis acid and B refers to Brønsted acid.

FTIR measurement at 200 °C are illustrated in Fig.7. The spectra reveal that ST/MCM-41 and d-ST/MCM-41 contain both Brϕnsted (at 1540 cm^{-1}) and Lewis (at 1445 cm^{-1}) acid sites [19], but only Lewis acidity can be observed for T/MCM-41. Several models have been proposed to explain the generation of acidity for TiO_2-SiO_2 and TiO_2/SiO_2, and usually the charge imbalance resulting from the difference in coordination number of Si from Ti in the mixed oxides was considered [1,2,4]. However, little agreement was reached due to the versatility of preparation methods and therefore properties of the materials. In this work, it can be speculated that the higher electronegativity of Si led to a charge transfer O→Ti at Si−O−Ti bonds, which improved the electron-accepting ability of surface Ti [1], and thus the Lewis acidity was produced on T/MCM-41. In addition, it is obvious that the improved Brϕnsted and Lewis acidities in ST/MCM-41 and d-ST/MCM-41 were generated from the introduction of inductive effect of S=O on the surface by sulfate treatment.

It is known that the mixture of α- and β-ionones could be produced using liquid acids as catalysts, and numerous by-products are difficult to avoid due to the complexity of the reaction [23,24]. In Table II, the conversion of pseudoionone and the selectivity of ionones obtained with the prepared materials and Amberlyst-15 as catalysts are presented, respectively. It can be seen that T/MCM-41 without sulfation is almost inactive for the cyclization reaction, while the other two sulfated samples show good activity, and ST/MCM-41 gave a result comparable with that of the commercial acid catalyst Amberlyst-15. This indicates that remarkable acid-catalytic activity can be produced by the sulfate treatment. It is notable that the catalytic performance of ST/MCM-41 is better than that of d-ST/MCM-41 which has much higher Ti and S content. This is distinct from the previous reports of sulfated crystalline metal oxides supported on MCM-41 [17-19], of which the acid-catalytic activity was improved with the content increase of crystalline metal oxides.

It has been reported that SO_4^{2-}/SiO_2 has hardly any acid activity due to the relatively higher electronegativity and low coordination number of Si, and the acidity of SO_4^{2-}/TiO_2 derives from octahedrally coordinative unsaturation of Ti in anatase phase [25]. In this work, with the formation of Si−O−Ti−O−S=O bonds on pore surface of ST/MCM-41, both the electronegativity difference of Si from Ti and the induction of S=O have an effect on Si−O−Ti bonds simultaneously to withdraw electron density of Ti in opposite directions, and thus desirable Brϕnsted and Lewis acidities and acid catalytic activity can be produced. For d-ST/MCM-41, however, it can be speculated that the activity mainly derives from the induction of S=O on the outer layer of the TiO_2 introduced by the second Ti grafting, which is similar to a sulfation effect on the surface of amorphous TiO_2 in tetrahedral coordination. Therefore, the d-ST/MCM-41 gave lower activity for the acid catalyzed reaction, although it possessed higher Ti and S content than ST/MCM-41. According to the characterization results, the sulfated surface TiO_2 in ST/MCM-41 are generally present in isolated units. It should be the specific surface structure of Si−O−Ti−O−S=O and the bilateral induction effect of Si and S=O that account for its better catalytic activity, in comparison to d-ST/MCM-41 with a second TiO_2 grafting.

DOI:10.1088/1674-0068/21/01/21-26

IV. CONCLUSION

ST/MCM-41 and d-ST/MCM-41 with well-ordered mesostructure were prepared by consecutive TiO_2 grafting onto pore surface of silica MCM-41 and sulfate treatment. T/MCM-41 without sulfation was also prepared for comparison. It was found that the sulfate treatment efficiently retarded the appearance of crystalline anatase and polymerization of TiO_2, and remarkably improved the acid-catalytic activity of the TiO_2 grafted silica MCM-41 for the cyclization reaction of pseudoionone, although the surface TiO_2 components were at low amount and in amorphous form. ST/MCM-41 without a second TiO_2 grafting possesses better catalytic activity as compared to d-ST/MCM-41, due to its well-dispersed surface species of Si−O−Ti−O−S=O with the bilateral induction effect of Si and S=O on Si−O−Ti bonds. It was shown that the sulfated forms of TiO_2 grafted mesoporous silica could be used as potential solid acid catalysts for reactions of bulky molecules.

V. ACKNOWLEDGMENTS

This work was supported by the National Basic Research Program of China (No.2007CB209705), and the Science & Technology Commission of Shanghai Municipality (No.06SN07115 and No.065211020).

[1] X. Gao and I. E. Wachs, Catal. Today **51**, 233 (1999).
[2] R. J. Davis and Z. Liu, Chem. Mater. **9**, 2311 (1997).
[3] J. R. Sohn and H. J. Jang, J. Catal. **136**, 267 (1992).
[4] J. Navarrete, T. Lopez, R. Gomez, and F. Figueras, Langmuir **12**, 4385 (1996).
[5] S. M. Jung, O. Dupont, and P. Grange, Appl. Catal. A: Gen. **208**, 393 (2001).
[6] T. Maschmeyer, F. Rey, G. Sankar, and J. M. Thomas, Nature **378**, 159 (1995).
[7] S. Zheng, L. Gao, Q. H. Zhang, and J. K. Guo, J. Mater. Chem. **10**, 723 (2000).
[8] M. Widenmeyer, S. Grasser, K. Köhler, and R. Anwander, Micro. Meso. Mater. **44-45**, 327 (2001).
[9] G. Galleja, R. van Gríeken, R. García, J. A. Melero, and J. Iglesias, J. Mol. Catal. A: Chem. **182-183**, 215 (2002).
[10] B. J. Aronson, C. B. Blanford, and A. Stein, Chem. Mater. **9**, 2842 (1997).
[11] Z. Luan, E. M. Maes, P. A. W. van der Heid, D. Zhao, R. S. Czernuszewicz, and L. Kevan, Chem. Mater. **11**, 3680 (1999).
[12] M. S. Morey, S. O'Brien, S. Schwarz, and G. D. Stucky, Chem. Mater. **12**, 898 (2000).
[13] S. Zheng, Z. P. Li, and L. Gao, Mater. Chem. Phys. **85**, 195 (2004).
[14] E. Brenna, C. Fuganti, S. Serra, and P. Kraft, Eur. J. Org. Chem. 967 (2002).
[15] E. E. Royals, Ind. Eng. Chem. **38**, 546 (1946).
[16] A. Croma, Chem. Rev. **95**, 559 (1995).
[17] T. Lei, W. M. Hua, Y. Tang, Y. H. Yue, and Z. Gao, Chem. J. Chin. Univ. **21**, 1240 (2000).
[18] C. L. Chen, T. Li, S. Cheng, H. P. Lin, C. J. Bhongale, and C. Y. Mou, Micro. Meso. Mater. **50**, 201 (2001).
[19] Q. H. Xia, K. Hidajat, and S. Kawi, J. Catal. **205**, 318 (2002).
[20] M. Grün, I. Lauer, and K. K. Unger, Adv. Mater. **9**, 254 (1997).
[21] T. Jin, T. Yamaguchi, and K. Tanabe, J. Phys. Chem. **90**, 4794, (1986)
[22] X. S. Zhao, G. Q. Lu, A. K. Whittaker, G. J. Millar, and H. Y. Zhu, J. Phys. Chem. B **101**, 6525 (1997).
[23] E. T. Theimer, *Fragrance Chemistry: The Science of the Sense of Smell*, Beijing: Science Press, 192 (1989).
[24] D. S. Guo, Z. F. Ma, Q. Z. Jiang, H. H. Xu, Z. F. Ma, and W. D. Ye, Catal. Lett. **107**, 238 (2006).
[25] T. Yamaguchi, Appl. Catal. **61**, 1 (1990).

DOI:10.1088/1674-0068/21/01/21-26